# Dimensioning a Compact Phased-Array Antenna for Millisecond Pulsars Detection & Timing

Alexis Rigaud, *Member, IEEE*
alexis@pulsr.sh

***Abstract*—This notice paper review the design and dimensioning of a compact phased-array antenna device used as a radiotelescope for millisecond-pulsar detection and timing.**

***Index Terms*—Radioastronomy, Phased-Array Antennas Design, Radiometer, Pulsars Detection, Pulsars Timing.**

## I. INTRODUCTION

IN this notice paper we reference the main equations for the demensioning and design of a compact receptive phased-array antenna that is able to detect millisecondes-class pulsars. First, a summary of the theory of radioastronomy instrumentation results are presented, from the observed source to the signal aquisition that are the main drivers for a radiotelescope device. Then we review the pulsar detection and timing constraints. Finally, we design a phased array antenna for such detection and present simulation results.

## II. RADIOASTRONOMY INSTRUMENTATION

Radioastronomy is the field of astronomicals observations through the radio waves. Ground-based radio observation were discovered possible by Karl Jansky in 1933, allowing the study of astronomical objects though the earth radio window, and therfore observations during daylight.

### A. Wave equation

A radio wave, also called electromagnetic wave (EM) is defined as a solution of the wave equation coming from the Maxwell equations governing the Electric $\boldsymbol{E}$ and Magnetic $\boldsymbol{B}$ fields in free space (with $c$ speed of light) :

$$\nabla^2(u) = \frac{1}{c}\frac{\partial^2}{\partial t^2}(u) \tag{1}$$

A solution is called the monochromatic plane wave :

$$u(t) = Ae^{i(\boldsymbol{k}r - \omega t)} \tag{2}$$

Where :

- $A$ is the amplitude, including a constant phase shift
- $\boldsymbol{k}r - \omega t$ is called the phase of the wave
- $\omega = 2\pi\nu$ is called the angular frequency
- $k = 2\pi/\lambda$ is called the angular wavenumber
- $\omega = kc$ that is posed when solving (1)

Thus allowing to write :

$$\lambda = c/\nu \qquad [\mathrm{m}] \tag{3}$$

### B. Flux Densities

When radio waves are considered as rays we can define the specific intensity $I_\nu$ as the rate of energy flowing out to an unit area, per unit solid angle and per unit frequency [2].

$$dE/dt = I_\nu \cos(\theta) d\Omega d\sigma d\nu \tag{4}$$

Where $\theta$ is the angle between the plane normal of the observation surface and the source. Assuming thermal equilibrium (TE), the flux density of a source $F_\nu$ is :

$$F_\nu = \int_\Omega I_\nu \cos(\theta) d\Omega \tag{5}$$

Radioastronomers use convenientely the Jansky unit : 1 [Jy] = $10^{-26}$ [$\mathrm{W\,m^{-2}\,Hz^{-1}}$].

### C. Thermal Processes

Radio emission brightness can be converted to thermal black-body temperatures equivalence, through the Plank law (where $k$ is the Boltzmann constant) :

$$B_\nu = \frac{2kT\nu^2}{c^2}\left[\frac{\frac{h\nu}{kT}}{exp(\frac{h\nu}{kT}) - 1}\right] \tag{6}$$

Using the approximation valid when frequencies are small $h\nu \ll kT$ yields to the Rayleigh-Jeans regime (RJ) :

$$B_\nu = \frac{2kT\nu^2}{c^2} = \frac{2kT}{\lambda^2} \tag{7}$$

Radioastronomers uses the resistor thermal noise power equivalence (called Nyquist-Johnshon noise) relation :

$$P_\nu = kT \qquad [\mathrm{W\,Hz^{-1}}] \tag{8}$$

Allowing radioastronomers to speak of brightness temperature of source, and to define temperatures as the equivalent power going trough a resistor.

$$T = P_\nu/k \qquad [\mathrm{K}] \tag{9}$$

Finally, the total noise power over a bandwith $\Delta_\nu$ is :

$$P = kT\Delta_\nu \qquad [\mathrm{W}] \tag{10}$$

### D. Atomospheric Attenuation

Due to atmospheric reflections and attenuations, the ideal radio window is above the kHz level and below 10 Ghz. Attenuations also depends on other factors, as the weather and elevation. The recommended values for approximations are summarized on an ITU document [1].

### E. Antennas

An antenna is a transducer that convert radio waves into EM guided waves traveling a metal conductor and vice-versa. The aperture area of an antenna is the principal plane surface that illuminates the antenna.

The power detected is function of the effective aperture area of the antenna (where the $1/2$ factor express one polarisation for an unpolarised source) cf [2] Eq. (3.35) :

$$P_\nu = \frac{1}{2} A_e S_\nu \qquad [\mathrm{W}] \quad (11)$$

We have the relationship between peak directive Gain $G$ and the effective aperture area $A_e$ holding :

$$A_e = \frac{\lambda^2}{4\pi} G \qquad [\mathrm{m}^2] \quad (12)$$

The antenna aperture efficiency is defined by the ratio between the effective aperture area and the physical aperture area $A_p$

$$\eta_e = A_e / A_p \quad (13)$$

The directivity of an antenna is expressed by its gain $G$ (where 1 is the isotropic case) cf [3] Eq. (7.10) :

$$G = 4\pi / \Omega \quad (14)$$

Beam area and aperture area are threfore linked with :

$$A_e = \lambda^2 / \Omega \qquad [\mathrm{m}^2] \quad (15)$$

The Half-Power Beam Width (HPBM or FWHM) is the total angle $\Delta_\phi$ of the radiation lobe at half maximum. It gives the resolution through the aperture (Rayleigh criterion) for an observation function of the main size $D$ of the aperture :

$$\Delta_\phi \propto \frac{\lambda}{D} \quad (16)$$

For radiotelescopes the beam is gausian [2] Eq. (3.118) :

$$\Omega = \frac{\pi}{4 \ln 2} \Delta_\phi^2 \qquad [\mathrm{sr}] \quad (17)$$

For planar arrays with HPMWs orthogonal [8] Eq. (2-26) :

$$\Omega \simeq \Delta_{\phi_x} \cdot \Delta_{\phi_y} \qquad [\mathrm{sr}] \quad (18)$$

The antenna temperature $T_A$ is the temperature generated by all sources in the antenna beam :

$$T_A = \frac{P_\nu}{k} = \frac{A_e}{2k} S_\nu \qquad [\mathrm{K}] \quad (19)$$

Where $dpfu$ (degree per flux unit) is an antenna gain performance factor.

$$dpfu = \frac{A_e}{2k} \cdot 10^{-26} \qquad [\mathrm{K\ Jy}^{-1}] \quad (20)$$

Therefore for any source in the beam :

$$T_s = dpfu \cdot S_\nu \qquad [\mathrm{K}] \quad (21)$$

For an compact source of temperature $T_s$ covering solid angle $\Omega_s$, we get the beam-filling factor contributing to $T_A$ [2] Eq. (3.56) :

$$\frac{T_A}{T_s} = \frac{\Omega_s}{\Omega_A} \quad (22)$$

### F. Guided EM Waves & Transmission Line Model

Through a waveguide radio wave are subject to one-dimensional traveling called transverse EM propagation mode (TEM), modeled with by a transmission line. The power of the wave is then the poynting vector cf [6] Eq. (11.1.11) :

$$P = \frac{1}{2} Re(\boldsymbol{E} \times \boldsymbol{H}^*) = \frac{1}{2} Re(V^* \cdot I) = \frac{1}{2} \frac{|V|^2}{Z} = \frac{V_{rms}^2}{Z} \quad (23)$$

Where $Z$ is the impedance of the line. When connecting differents element, the impedances shall be matched to avoid reflexions and attenuations.

This result show that the power of the radio wave can be capture by the averaged voltage squared outputed by the antenna.

### G. Signal Processing

Assumptions on the signals to be processed are :

- Are stationary random processes and ergodic
- Are band-limited (over the bandwith $\Delta_\nu$)
- Have white noise spectrum (Gaussian)
- Pulsars signals are considered cyclostastionary.

Sampling rate shall be at least twice the bandwidth (Sampling theorem). Real-valued signals can be extended on the complex plane trough the Hilbert transform [7] :

$$S(t) = Re\left( [I(t) + iQ(t)]\, e^{i\omega t} \right) \quad (24)$$

Where $S_A(t) = I(t) + iQ(t)$ is called the baseband signal.

### H. Radio Wave Polarisation

Radioastronomers measures all the Stokes parameters $(I, Q, U, V)$ to recover the full wave emmitted by celestial objects. In the following set of equation, $E_X$ is an averaged voltage measurement one one linear polarisation direction ($X$-axis), and $E_Y$ is corresponding $90\,\deg$ perpendicular linear polarisation measurement ($Y$-axis) cf [5] Eq. (4.2) :

$$\begin{aligned} I &= E_X {E_X}^* + E_Y {E_Y}^* \\ Q &= E_X {E_X}^* - E_Y {E_Y}^* \\ U &= E_X {E_Y}^* + E_X {E_Y}^* \\ iV &= E_X {E_Y}^* - E_X {E_Y}^* \end{aligned}$$

Jones and Mueller matrix are used to correct effects affecting the reception of the radio waves (faraday rotation, effect of the RF chain) cf [5] Eq. (5).

The parameters I reflect the total flux density (including polarisation), whereas $I_p = \sqrt{Q^2 + U^2 + V^2}$ is the polarised-only flux density of the wave. The degree of polarisation is threfore cf [3] Eq. (2.58) :

$$p = I_p / I \quad (25)$$

### I. The Receiver

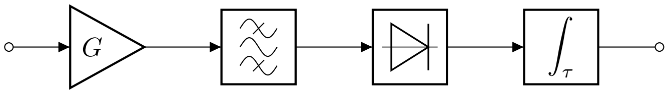


The square law detector allow the to capture the power of the signal over an integration time $\tau$.

$$P_{rms} = \int_{t-\tau/2}^{t+\tau/2} V(t)^2 dt \tag{26}$$

Using (10), this give the *radiometer equation* cf [3] (p83) :

$$\frac{\Delta T}{T} = \frac{K}{\sqrt{\Delta_\nu \tau}} \tag{27}$$

With $K$ a combination function of the type of radiometer and the ADC performance :

- $K = 1/\sqrt{2}$ (two polarisation used instead of one)
- $K = 1$ (Total power receiver)
- $K = 2$ (Switched Dicke receiver)
- $K = \sqrt{2}$ (Correlation receiver)
- $K = 2.21$ (One-bit ADC)
- $K = 1.58$ (Two-bit ADC)

Taking into account the gain fluctuation $\Delta G$ we get the *practical radiometer equation* cf [3] Eq. (4.65) :

$$\frac{\Delta T}{T} = K \left[ \frac{1}{\Delta_\nu \tau} + \left( \frac{\Delta G}{G} \right)^2 \right]^{-1/2} \tag{28}$$

Highlighting that gain stability is an critical parameter of the receiver chain.

### J. Reciever Temperature

To compute an RF-chain receiver temperature, the addition of band-limited signals with stages gains $G_i$ is as follow (Friis formula) :

$$T_r = T_1 + \frac{T_2}{G_1} + \frac{T_3}{G_1 G_2} + ... \tag{29}$$

Temperatures $T_i$ can be deduced from Noise Figure (NF) with the use of :

$$T = 290 \cdot (NF - 1) \tag{30}$$

Theoretical minimum receiver temperature is ([3] 4.49) :

$$\min(T_r) = \frac{h\nu}{k} \tag{31}$$

### K. System Noise Temperature $T_{sys}$

The system noise temperature is the total noise seen by the system cf [2] Eq. (3.150), that includes all contributions to the measurements :

$$\begin{aligned} T_{sys} = {} & T_{cmb} + T_{sky} + T_{source} \\ & + T_{atm} + T_{spill} + T_r + ... \end{aligned}$$

Where folowing temperatures are expressed in Kelvin [K]:

- $T_{cmb} = 2.73$ (cosmological background)
- $T_{sky} = 10(\frac{\nu}{1.4e9})^{-2.7}$ (sky brightness) cf [2] Eq. (3.151)
- $T_{source} = S_{source} \cdot dpfu$ (observed source) cf Eq. (21)
- $T_{atm} = 0.04 \cdot 290 \cdot \csc(\theta)$ (atmospheric) cf [2] Eq. (2.44)
- $T_{spill} = 10$ (spillover refraction typ. value)
- $T_r$ (noise temperature of the reciever)

### L. Sensitivity

Limiting flux density of a point source is [4] Eq. (p35) :

$$\Delta S_{min} = S/N \cdot \frac{2k}{A_e} \cdot T_{sys} \cdot K \cdot \frac{1}{\sqrt{\Delta_\nu \tau}} \tag{32}$$

With $S/N$ is the minimum signal-to-noise ratio (SNR) value to allow detection, typically from 3 to 5.

### M. Figure of merit

The sensitivity of a radio-telescope can be expressed as an “A over T” factor :

$$A_e/T_{sys} \qquad [\mathrm{m^2\,K^{-1}}] \tag{33}$$

Or with the System Equivalent Flux Density (SEFD) :

$$T_{sys}/dpfu \qquad [\mathrm{Jy}] \tag{34}$$

## III. Pulsar Detection & Timing

Pulsars are fast-rotating neutrons stars that emit a continuous radio beam. When the beam cross the observer (lighthouse effect), the pulsars signals are seen as short and weak radio burst that repeats precisely. The cyclostationary nature allows to implements specific signal processing techniques cf [9].

### A. Spectra

Among the pulsar population, milliseconds-class pulsars are best observed in the 1.4 GHz Band cf [12] (chap. 2). The flux density decrease with frequency with a power-law fashion, were spectral index $\alpha$ indicates the steepness (typ. $\alpha \approx -2$) :

$$S_{mean}(\nu) \propto \nu^\alpha \tag{35}$$

Therefore, applied to 1.4 Ghz :

$$S_{mean} = S_{1400} \left( \frac{\nu}{1.4 \cdot 10^9} \right)^\alpha \tag{36}$$

### B. Pulsar Radiometry

Following Lorimer & Kramer (in [10] A1.17) we can divide the observation between an OFF period (no pulse) and ON period (pulse) with :

- W = pulse width (ON)
- P = pulse period (ON + OFF)

We get relationship with the mean flux density emitted by a pulsar and the peak flux density though the duty cycle :

$$S_{mean} = S_{peak} \left( \frac{W}{P} \right) \tag{37}$$

And applied to the radiometer equation, eq. (32) becomes :

$$\Delta S_{min} = S/N \cdot \frac{2k}{A_e} \cdot T_{sys} \cdot K \cdot \frac{1}{\sqrt{\Delta_\nu \tau}} \cdot \sqrt{\frac{W}{(P - W)}} \tag{38}$$

### C. Folding & Average Pulse Profile

The average pulse shape profile is computed with the coherent addition of observed individual pulses (folding), as described in [10] Eq. (7.1).

This improves detection (for the average pulse) by a factor of $1/\sqrt{N_p}$ with $N_p$ the number of folded pulses cf [13] Eq. (17.5.4).

Moreover, recent advanced radio pulsar processing techniques such as filtering of the signal with an adapted filter based on the pulse profile have been explored to improve the detection of the individual peaks [11].

### D. ToA Pulse Fiting

The model for timing-of-arrival (ToA) recovery is as follow, see [15] Eq. (4.1) :

$$P(t) = a + b \cdot s(t - c) + g(t) \tag{39}$$

Where $s(t)$ is the pulsar profile, $g(t)$ is a gaussian white noise, and $a, b, c$ are the fitted constants. With the average pulse shape of a pulsar known, it is possible to cross-correlate the signal and extract indidivual pulses ToA = $c$.

Finally, the uncertainty on the ToA of the individual pulses can be written as cf [10] Eq. (8.2)

$$\sigma_{ToA} \simeq \frac{W}{(S/N)} \tag{40}$$

### E. De-Dispersion

Dedispersion is the process of removing the dispersion due to Inter-Stellar Medium (ISM) scattering. The coherent de-dispertions techniques (through a chirp signal) have been succesfully used to remove the ISM effects cf [15].

### F. Solar System Barycentric (SSB) Correction

Once ToA are extracted, they can be corrected toward earth position relative to the Solar System Barycentric (SSB) center, the pulsar ephemeris (ICRS frame) and the relativistic effects back to the inertial frame of reference of the observation. The overall process is detailed in [18].

### G. Pulsar Timing Model

Pulsar Timing Model allow to recover time-residual as folow (with taylor expansion at epoch $t_0$), with $\nu = 1/P$ see [16] Eq. (5.13) :

$$N = \nu_0(t - t_0) + \frac{1}{2}\dot{\nu}(t - t_0)^2 + \frac{1}{6}\ddot{\nu}(t - t_0)^2 + ... \tag{41}$$

The process of ToA extraction, correction and pulse numbering is called pulsar timing cf [17] (chapter 6).

### H. Pulsar Polarimetry

The rotating vector model (RVM) can be used to model the pulsar EM emission and gain insigh to the geometrical beam of the pulsar.

### I. Tools

Serveral usefull software tools are adapted for pulsar radio-astronomy and are listed here, such as the pulsar catalogue from ATNF (psrcat), file format adapted to pulsar measurements storage and analysis (psrfits), a software suite for pulsar detection and analysis (presto), and pulsar timing software (tempo2 & pint). Moreover, a pulsar signal generator exists (psrsigsim).

## IV. Phased-Array Antenna Design

We now design a squared planar phased-array antenna composed of $N \cdot N$ elements, spaced by $d = \lambda/2$, with the parameters :

- Uniform Planar Array (UPA)
- $f_c = 1413.5$ [MHz] (center frequency)
- $\Delta_\nu = 27$ [MHz] (bandwitdh)
- $d = \lambda/2 = 10.60$ [cm] (element spacing)
- $N = D/d = 32$ (number of linear elements)
- $D = 3.393$ [m] (linear size)
- $N^2 = 1024$ (total number of elements)

### A. HPBW (one-axis)

Considering an elevation at zenith $\phi_0 = 90\,\mathrm{deg}$, a rectangular broadening factor $b = 1$ and elements spacing of $d = \lambda/2$, the HPBW for one axis is, cf Orfanidis [6] Eq. (22.10.3) :

$$\Delta_{\phi_x} = 1.772/N \qquad [\mathrm{rad}] \tag{42}$$

### B. Directivity & Efficiency

For a uniform linear array (ULA), the directivity gain at broadside is $D = N$, see [6] (22.8.3). The directivity gain $G$ of a UPA is deduced from (ULA) with, cf [8] (6-103) :

$$G = \pi D_x D_y \sin\phi_0 = \pi N^2 \sin\phi_0 \tag{43}$$

Along with eq. (12) we deduce the effective aperture area :

$$A_e = \frac{\lambda^2}{4\pi} G = \left(\frac{\lambda}{2} N\right)^2 \sin\phi_0 = D^2 \sin\phi_0 \tag{44}$$

Therefore, as $A_p = D^2$ the effective aperture efficiency $\eta_e$ is simply the elevation of the observation $\eta_e = \sin\phi_0$. We get a theoretical gain of 35 dBi at broadside (zenith) and of 32 dBi near enfire (30 deg. elevation). The directivity gain of the elements shall be added to get to total gain (here neglected).

## V. Conclusion

A Python script (available here [1]) based on the set of results presented in this paper show the detection of a pulsar possible for a 11.5 [$\mathrm{m}^2$] patch phased-array planar antenna.

Such a compact radio-telescope open industrial applications though pulsar pulses timing observation (synchronisation & chronometry) [12] and the foreseen usage of a pulsar timescale [19]. It would act as a reliable, resilient and stable source of time, and provide an alternative to time & synchronisation based on GNSS or atomic solutions.

[1] https://github.com/pulsr-software/PulSR

TABLE I
SIMULATION RESULTS

| Name | Unit | Value |
|---|---|---|
| center freq. | [Hz] | = 1413500000 |
| bandwidth | [Hz] | = 27000000 |
| sampling freq. | [Hz] | = 54910633 |
| integration time | [s] | = 3600.000 |
| Phased array lenght | [m] | = 3.393 |
| Physical Aperture | $[m^2]$ | = 11.516 |
| Antenna gain | [dBi] | = 34.656 |
| Tsys | [K] @freq | = 42.001 |
| DPFU | [K Jy$^-1$] | = 0.004 |
| sensitivity | $[m^2$ K$^-1]$ | = 0.249 |
| SEFD | [Jy] | = 11089.905 |
| Resolution | [deg] | = 3.173 |
| Location | [ASCII] | = Lyon |
| Date | [ISO8601] | = 2022-11-18T15:03:42.628 |
| Altidude | [deg] | = 65.251 |
| Azimuth | [deg] | = 164.871 |
| Name | [ASCII] | = J1939+2134 |
| Period | [ms] | = 1.558 |
| duty cycle | [%] | = 0.025 |
| Pulsar peak | [mJy] | = 606.686 |
| Noise Level | [mJy] | = 25.152 |
| Pulsar min (3dB) | [mJy] | = 11.964 |
| Pulsar mean | [mJy] | = 14.877 |
| SNR psr peak | [dB] | = 5.718 |
| $\sigma_{ToA}$ | [us] | = 10.240 |

## REFERENCES

[1] ITU-R P.676-11, Attenuation by atmospheric gases, 09/2016.
[2] Condon & Ransom, Essential Radio Astronomy, 2016.
[3] Wilson & Rohlfs, Tools of Radio Astronomy, 2013.
[4] Burke & Graham-Smith, Introduction to Radio Astronomy, 2009.
[5] Heiles, A Heuristic Introduction to Radioastronomical Polarization, 2001.
[6] Orfanidis, Electromagnetic Waves and Antennas, 2016.
[7] Lyons, Generating Complex Baseband and Analytic Bandpass Signals, 2011.
[8] Balanis, Antenna theory: analysis and design. 2016.
[9] Demorest. Cyclic spectral analysis of radio pulsars, 2011.
[10] Lorimer & Kramer, Handbook of Pulsar Astronomy, 2004.
[11] Heusdens & al, Match filtering approach for signal acquisition in radio-pulsar navigation, 2012.
[12] ITU-R RA.2099-1, Radio observations of pulsars for precision time-keeping, 2013.
[13] GMRT, Low Frequency Radio Astronomy (Blue Book), 2003.
[14] Escudeiro, Digital Signal Processing System for Pulsar Signal Reception, 2015.
[15] Stairs, Pulsar Observation II. - Coherent Dedispersion, Polarimetry and Timing, 2002.
[16] Lyne & Graham-Smith, Pulsar Astronomy, 2012.
[17] Manchester & Taylor, Pulsars, 1977.
[18] Edwards & al. TEMPO2, a new pulsar timing package – II. The timing model and precision estimates, 2006.
[19] Hobbes & al., A pulsar-based timescale from the International Pulsar Timing Array, 2019.